ELSEVIER

Nuclear Instruments and Methods in Physics Research B 130 (1997) 692–699

NIM B
Beam Interactions with Materials & Atoms

Tracing fossil and present day fluids in rocks: application of the nuclear microprobe

M. Volfinger [a,*], C.G. Choï [b], C. Ramboz [a], M. Aïssa [c], M. Edon [a]

[a] *CRSCM-CNRS, 1A rue de la Férollerie, 45071 Orléans Cedex 2, France*
[b] *CERI-CNRS, 45071 Orléans Cedex 2, France*
[c] *Geology Department, Meknès University, Meknès, Morocco*

Abstract

Geological fluids contain water, chlorides and Na as major components, and metals, CO_2 gas and CH_4 gas as minor or major components. Quantitative analysis of geological fluids in fluid inclusions and hydrothermal minerals is vital to the characterization of fluid–rock interactions. The presence and quantity of trace and minor elements can be determined in fluid inclusions and minerals by Proton-induced-X-ray-emission (PIXE) and Proton-induced-gamma-ray-emission (PIGE) with EDS analysis, based on computer-aided interpretation of X-ray spectra. A feature of the PIXE-PIGE method is the long range (deep penetration) of protons in light matrices, which allows near-surface inclusions to be analysed. The applications presented here concern samples from submarine hydrothermal deposits (Red Sea, Lau Basin), and from skarns in Central Morocco. In submarine hydrothermal processes, PIXE data show trace-element-bearing-mineral(s) in assemblages with bulk geochemical anomalies, e.g. Co- and Pb-contents in the 1000 ppm range in chalcopyrite from the Hine-Hina field, Lau basin. PIXE data for high T chimneys of the Atlantis II deep record trace element perturbations due to boiling. Hypersaline magmatic fluids in the Sn-skarns of El Hammam contain more than 1000 ppm Cu and Pb but no Zn. A Sn-borate, nordenskiöldine, has been identified in the high T-skarns, trapping a Li-bearing concentrated brine. © 1997 Elsevier Science B.V.

1. Introduction

The composition and rheology of rocks are affected by the presence of fluid phases during their evolution. Geological fluids equilibrate with various magmatic, metamorphic or sedimentary reservoirs. Reservoir fluids migrate down pressure gradients or along permeability barriers and they react with wall-rocks along their path. The ability of fluids to undergo abrupt chemical changes through decompression, phase separation or fluid mixing favors fluid (super)saturation and the deposition of ore-bearing minerals in economic amounts. To reconstruct the intensive and extensive parameters during the evolution of rocks, one must quantitatively analyse the major and trace element compositions of minerals and related fluid inclusions (FI). Such data provide constraints on fluid-flow pulses because the partitioning of major and trace elements between a mineral and a fluid, or between several minerals, is a function of P, T and composition of the fluid. These partitioning relations can be determined experimentally. The trace element compositions of fluids or minerals can discriminate between magmatic or hy-

* Corresponding author. Fax: +33 0238636488; e-mail: volfinge@cnrs-orleans.fr

PII S0168-583X(97)00266-8

drothermal sources. However, due to the small size of FI, the kinetics of silicate growth and the diffusion rates of elements through minerals, the analysis of major and trace elements in geological solids or fluids has to be performed in the micrometer range in order to permit accurate thermobarometric or geochemical interpretations.

Chemical analyses of solids at a micrometer scale can be made using both the electron microprobe (EPMA) and the PIXE microprobe. The PIXE method is non-destructive, provided that the current density on the target is low. Unlike EPMA, the PIXE microprobe allows trace elements to be analysed by EDS at ppm level. The light elements (Li, B), undetectable by EPMA, can be analysed, by coupling the PIGE method with PIXE.

A significant potential advantage of the PIXE-PIGE microprobe compared with EPMA is the penetration depth of protons through solids (e.g. about 70 μm in silicates at 3 MeV). X-rays emitted from less than about 20–30 μm, depending on photon energy, can be detected in a silicate. For γ-rays originating from the whole volume irradiated by protons, the attenuation through solids is negligible. Because of the long range of protons, the PIXE-PIGE method has been applied to characterizing the ion content of FI situated at 10–30 μm depth in a mineral [1,2]. It is complementary to other non-destructive techniques like microthermometry and Raman microspectrometry, which allow volumetric properties, bulk salinity and volatile content of the trapped fluids to be characterized.

We present here applications of the nuclear microprobe in characterizing geological fluids, either fossil fluids from magmatic environments or modern fluids from the oceanic crust. We have determined the halogen and metal contents of hydrothermal minerals (sulfides, sulfates and silicates), and we have analysed trapped fluids in silicates.

2. Analytical methods

The nuclear microprobes of two French laboratories were used.

The apparatus from the CERI / CNRS at Orléans consists of a 3 MV, one stage vertical KN 300 Van de Graaff accelerator. The quadrupole of the PIXE line allows the proton beam to be focused at 30×60 μm^2 [3]. A maximum current density of 0.25 $pA/\mu m^2$ is obtained, which allows the FI to be preserved after irradiation. In general, the beam spot is larger than the size of the analysed FI. The charge (Q) received by the occluded fluid can be estimated either from the ratio of the irradiated part of the inclusion surface area to that of the beam spot, or adjusted using the known concentration of an element, e.g. Cl. The intensity of the proton beam on the target is measured using a chopper calibrated relative to a Faraday cup placed behind the sample holder. We used two detectors oriented at 45° from the beam and the target surface: a 10 mm^2 Si-Li detector and a 30 mm^2 LeGe detector. Their resolutions at 5.9 keV are 148 and 160 eV, respectively. The latter detector is used to characterize fluorine by its characteristic γ-ray emission at 110 keV and to analyse the K X-rays of heavy elements, mainly REE [4]. The visualization system, which magnifies at $200\times$, is placed on the beam path and must be taken off during irradiation.

The nuclear microprobe at the Pierre Süe Laboratory at Saclay (CEA-CNRS) [5] consists of a 4 MV single stage horizontal accelerator. The focussing system of the PIXE-PIGE line (quadrupole and collimation slit) permits a 1×1 μm^2 beam to be obtained. We have used current densities of 10 $pA/\mu m^2$ with beam sizes ranging from 10 to 100 μm^2. Two detectors, each one placed at 45° from the beam and the sample surface, allow the X- and γ-ray emissions to be analysed using a Si-Li (resolution of 180 eV at 5.9 kev) and an intrinsic Ge detector (relative efficiency of 80%). The visualization system consists of a microscope with a hollow objective which enables the target to be observed with a $400\times$ magnification during irradiation.

X-ray spectra were quantitatively interpreted using the GUPIX program [6]. Trapped fluids in crystals can be treated using the multi-layer procedure in this program, provided that the depth to the top of the cavity in the host mineral and the FI thickness are known [7]. These two parameters were estimated using a DMR Leitz microscope equipped with a motorized stage, which allows the vertical positioning to be reproduced at ± 1 μm. For a 10 μm-deep FI in quartz, the relative uncertainty on the roof

thickness results in an uncertainty of 35% on Cl, and of ~4% on the concentrations of elements heavier than Fe (RX > 6 keV) [2,8]. The mean depth of the cavity in the host can also be adjusted from the Kα/Kβ intensity ratio of a given element (Cl, Ca, Fe, etc.) [2]; however the Kα and Kβ peaks of Cl are measurable only in salt-rich FI. A relative uncertainty on the Kα/Kβ ratio of 10% yields an uncertainty of ~3 μm on the quartz roof thickness, which only allows confirmation of the optical measurement. When the beam is larger than the FI surface area, the adjusted depth corresponds to that of an equivalent FI with a flat shape. The trace metal contents of FI are normalized to Cl, and the Cl content is evaluated independently from the bulk salinity determined by cryometry [9]. The uncertainty on microthermometry-derived Cl contents mainly arises from an interpretation based on simplified systems. It can be estimated at < 5%, given that microthermometric data are now currently interpreted with reference to ternary systems (H_2O-NaCl-$CaCl_2$, H_2O-NaCl-CO_2, H_2O-NaCl-KCl, etc.) and that geological fluids are Na- and Cl-dominant [10].

γ-ray spectra result from nuclear reactions on light elements of the target (Li, Be, B, F, Na, etc.). Their concentrations are determined with respect to standards analysed under the same conditions [11]. Corrections to account for the nature of the analysed matrices are applied, following the method of Ishii et al. [12]. The determination of the light element content of trapped fluids from γ-ray emission is currently qualitative. Quantification will require the use of Li-B-F-Na-Mg-Cl-bearing FI as standards, which can be synthesized hydrothermally at high P and T in the laboratory.

3. Oceanic vent fields

Volcanogenic and sedimentary exhalative massive sulfide (MS) deposits are important sources of base metals. Such deposits form by hydrothermal circulation through volcanic rocks and sediments, respectively. Zones of present day fluid venting at the seafloor are direct analogs of ancient MS deposits. Modern vents have been actively explored to evaluate the nature and spatial distribution of major and trace elements in MS. Convection through basaltic crust yields Cu-enriched ores whereas convection through mixed basaltic and felsic rocks (e.g. in back-arc settings) or sedimentary rocks produces Zn, Pb, Ag, Sn and Sb enriched ores [13,14]. Additionally, fluid boiling and mixing control economic gold deposition at the seafloor [15,16]. We present some PIXE analyses of submarine sulfate-sulfide chimneys from two young oceanic spreading zones (< 1 Ma):

Table 1
Mineralogy, bulk Au contents and formation conditions of the sulfate-sulfide assemblages studied (after [14,17,18,20])

Hine Hina vent (Lau Basin)		SW basin of Atlantis II deep, core 268	
NL 16-02		Level 1120	Level 980
Stage 1	Stage 2	*anhydrite-sulfide* poor	*barite-sphalerite* (+*anhydrite*)
chalcopyrite	*barite*, marcassite, Fe-poor-sphalerite		
	Au 0.69 ppm	Au 0.4–2 ppm	Au 20–31 ppm
	T ~ 230–190°C saline NaCl-$MgCl_2$ boiling fluid, mixing with sea-water	T ~ 390–150°C 4 to 8 M NaCl fluids boiling, minor mixing with sea-water	T ~ 400–150°C 4 to 8 M NaCl fluids, metastable discharge

Italicized minerals have been investigated by PIXE.

the Lau back arc basin in the Pacific Ocean, and the Red Sea sedimented ridge. The Vai Lili and Atlantis II vent fields from these two spreading centers are characterized by the discharge of high temperature (> 340°C), boiling fluids [17,18]. They host the most highly gold-mineralized seafloor samples yet found (> 30 ppm [13,19]).

The three barite-anhydrite-sulfide ores studied have differing parageneses, degrees of bulk gold enrichment and origins (Table 1). Sample NL16-02 is representative of the Cu-Fe massive sulfides from the low gold Hine Hina boiling field in the southern Lau Basin [14,17]. It is a polyphase assemblage, where gold is concentrated in pyritic ores from stage 2 [14]. The two samples from Central Red Sea are high T sulfate-sulfide veins typical of geyser brine discharge in the SW basin of Atlantis II deep [20]. The level 1120 sample, anhydrite-dominated and with a low sulfide- and gold-content, is typical of the boiling zone at the base of core 268. By contrast, level 980 has a massive mineralization of Zn, Cu, Ag, Sb, Pb and Au [20]. It is thought to have formed by quenching of high temperature ($T \leq 400$°C), superheated hydrothermal fluid at the subseafloor, with minor seawater mixing [21].

Barite and relict chalcopyrite in barite from *sample NL16-02* were analysed using a polished section. Barite shows trace amounts of Fe, Cu and Sr (Table 2). For the chalcopyrite analysis, the X-ray spectrum was interfered with by X-rays from an underlying barite crystal. Major and trace elements in chalcopyrite (Fe, Cu and Co, Pb) were estimated using the multi-layer procedure in GUPIX, assuming that all strontium and barium were in barite and neglecting its Fe and Cu contents (220 et 120 ppm; Table 2). A 2% relative uncertainty on Sr yields a 10% relative uncertainty on the thickness of the overlying sulfide, which in turn induces an additional 10% relative uncertainty on the trace metal contents of the sulfide. NL16-02 chalcopyrite has a high Co content (~ 1500 ppm), which is typical of high T Cu-rich East Pacific Ridge chimneys [13,22]. It plots close to the Pb-Co field of basaltic ridge ores, which is consistent with the Hine Hina field having a basalt-dominated geochemistry [14]. Note that the Fe/Cu in barite is around twice the Fe/Cu ratio of the sulfide it replaces (Table 2).

The 980 and 1120 samples of the Atlantis II deep core analysed by PIXE are sulfate concentrates consisting of a fine grained sulfate-sulfide assemblage. Anhydrite and barite were analysed separately in both cases, but sulfides were always analysed with barite or anhydrite under the 30×60 μm^2 proton beam because of their small size. As previously, Sr was allocated to sulfates and trace metals to Zn-Fe-sulfides (Table 2). A Zn–Cd plot of bulk sediment analyses permits the boiling zone to be discriminated from the rest of the core [13]. Zn–Cd data for sulfate-sulfide mixtures allow sample 980 in the 'normal sample' field to be distinguished from sample 1120 in the highly scattered boiling field (Fig. 1). This is because there is no Zn- and Cd-bearing mineral other than sphalerite in most core 268 sediments, and this mineral is analysed as solid inclusions in sulfates. PIXE analyses of samples 980 and 1120 thus confirm the proposed interpretation of a contrasted origin for these two samples. Note that level 980 anhydrite which co-precipitates with barite is barium-free, whereas anhydrite from the barite-free 1120 level contains 750 ppm Ba.

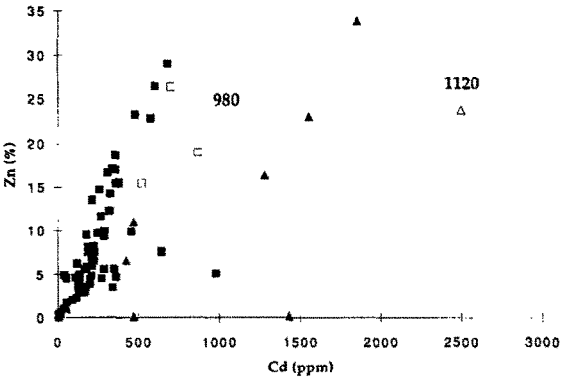

Fig. 1. Zn–Cd correlation diagram for metalliferous sediments in an Atlantis II deep core (Red Sea). Black symbols are bulk chemical analyses after [13]. Sediments with associated boiling fluids in FI (triangles) are distinguished from the rest of the core (squares). Empty symbols are PIXE analyses of sulfate-sulfide assemblages. Level 980 is a massive mineralization associated with non-boiling fluids; level 1120 is a poorly mineralized sample typical of the boiling zone (see text and [18,20,21]).

4. Chronology of skarn parageneses

Skarns are metasomatic rocks that result from volatilization reactions occurring in carbonate rocks

Table 2
PIXE/PIGE data for mineral matrices and FI from submarine hydrothermal and skarn environments

Element	barite Red sea	sulfide Red Sea	anhydrite Red Sea	anhydrite Red Sea	sulfide Red Sea	barite Lau basin	chalcopyrite Lau basin	diopside El Hammam		presumed malayaite El Hammam		
	980 cm	980 cm	980 cm	1120 cm	1120 cm					EPMA	PIXE/PIGE	
	Matrices							Matrix	FI	Matrix	Matrix	FI
S %		nc	24.8 (0.1)	nc	nc							
Cl%			0.15 (0.02)	0.26 (0.05)								nd
Ca %			26.7 (0.1)	30.35 (0.05)				17.6 (0.2)		15.55	15.0 (0.2)	
Ti												
V												
Mn %		0.33 (0.02)			0.34 (0.02)			0.53 (0.05)				
Fe %		10.6 (0.06)	0.159 (0.002)	nc	9.28 (0.05)	0.022 (0.004)	31.26 (0.03)	2.36 (0.05)				
Co					930 (200)		1500 (600)					
Ni		470 (60)	180 (24)		420 (50)							
Cu		1150 (150)	1090 (15)		430 (60)	120 (15)	33.94 (0.03)	25 (10)	6250 (1000)			
Zn		48.7% (0.06)			59.7% (0.1)			300 (60)	≤ lod 1000			
Ga												
As		100 (20)						≤ lod 30				
Br												
Rb												
Sr	9600 (100)		765 (33)	1335 (70)		7600 (90)						
Zr												
Ag		380 (100)			420 (120)							
Cd		1740 (150)			5800 (200)							
Sn %								≤ lod 400 ppm		43.1	43.9 (0.9)	
Ba	51.3% (0.7)			750 (150)		58.6% (1.2)						
Au												
Pb		570 (200)			260 (130)		1070 (110)	≤ lod 70	1600 (600)			
Li												y
B %											5.83 (0.15)	y
Na												y

Concentrations are given in ppm, except for specified elements in wt%. Figures in parentheses are 1 standard deviation. The presumed malayaite has been identified as nordenskiöldine by PIXE/PIGE analysis, its EPMA analysis is also given.
nd = not determined; nc = not calculated; y = detected in FI with γ-ray emission; lod = limit of detection.

(dolomites, marbles) in contact with a magmatic intrusion. In the Sn-W-F district of El Hamman (Central Morocco), subeconomic Sn-W-B-bearing skarns are developed in calc-schists of Upper Visean age (340 Ma) at the top of a buried granitic intrusion. Three stages were previously recognized, summarized in Table 3 [23].

A geochemical investigation of skarn minerals and related FI was undertaken using SEM, EPMA, microthermometry and Raman microspectrometry. In particular, the thermobarometric formation conditions of the different stages were determined, together with the bulk composition of the fluids (Table 3; [24]). Due to the ascent of the batholith, W-skarns were firstly formed at temperatures of contact metamorphism in the presence of low-density, low-salinity, CH_4-bearing fluids. Sn-bearing skarns then developed as a result of the infiltration of dense and hypersaline fluids at magmatic temperatures. Both these early skarns were formed at a similar pressure of around 1 kbar. Finally, B-skarns were formed at much lower P and T from low salinity fluids.

PIXE-PIGE results were obtained on millimeter-scale mineral grains from stage 2 diopside and malayaite. *The diopside* matrix was found to contain heterogenous amounts of Fe, Cu and Zn. A high temperature FI, 28 ± 1 μm thick and 25 ± 2 μm deep in diopside, yielded additional peaks for Cu and Pb. In order to estimate the minor and trace element content of the fluid, the theoretical X-yields of these elements originating from the overlying host were calculated using the GUYLS procedure of the GUPIX package [2,6]; the results are given in Table 2. Boron was detected neither in diopside nor in the related fluid. Cu and Pb are present in the fluid at the 6000 and 1500 ppm level, respectively, whereas sphalerite (ZnS) is dominant over galena and chalcopyrite (PbS and $CuFeS_2$) in the wall-rock [23]. For magmas of felsic composition, the partition coefficients of Pb and Zn between vapor and melt are in favor of the

Table 3
Paragenetic sequences and pressure–volume–temperature–composition characteristics of FI in El Hammam skarns (after [23,24])

		METAMORPHIC W-SKARNS (stage 1)	MAGMATIC Sn-SKARNS (stage 2)	HYDROTHERMAL B-SKARNS (stage 3)
wo	$CaSiO_3$	———		
di	$CaMgSi_2O_6$	———		
fs	$Ca(Fe,Mg)Si_2O6$	———		
sch	$CaWO_4$	———		
Sn-ga	$Ca_3(Fe,Sn)_2Si_3O_{12}$		———	
ma	$CaSnSiO_5$		———	
Mn-he	$Ca(Fe,Mn)Si_2O_6$		———	
no*	$CaSn(BO_3)_2$		———	- - -
axi	$Ca_2(R^{2+})_3Al_2BO_3Si_4O_{12}(OH)$			———
da	$CaBSiO_4(OH)$			———
	Fluid chemistry	H_2O-CH_4 <2wt% NaCl d<0,31	hypersaline brine 40 to 55 wt% NaCl	6 to 13 wt%NaCl
	P-T conditions	500°-550°C 1 kb	570°-630°C 1 kb	360°- 420°C 250- 375bar

wo = wollastonite; di = diopside; fs = ferrosilite; sch = scheelite; Sn-ga = Sn-bearing garnet; ma = malayaite; Mn-he = manganiferous hedenbergite; no = nordenskiöldine; axi = axinite; da = datolite.
* this study (see text).

vapor, and the partition coefficient of Zn is greater than that of Pb [25]. The Zn-poor nature of the magmatic fluid in diopside therefore implies either that Zn has a metamorphic origin, or that the magmatic brine had precipitated ZnS before trapping.

The presumed malayaite analysed by EPMA is silica-free and Ca- and Sn-rich (Table 2). This material could be burtite ($CaSn(OH)_6$) or nordenskiöldine ($CaSn(BO_3)_2$). Raman spectrometry shows that it is a OH-free mineral and PIGE revealed 18.8 wt.% B_2O_3, using a boron-rich silicate glass as a standard. These results are thus the first reported occurrence of nordenskiöldine in El Hammam skarns. An elongate FI (60 μm long and 12–15 μm large) with 3 to 4 daughter minerals was analysed in nordenskiöldine. Na and Li were detected by PIGE and one cubic solid was identified as NaCl by the characteristic γ-emission of Na. The other solids, Na-free, could be borates but they cannot be distinguished easily from the host. A Raman spectrum was obtained on one solid but it could not be interpreted for lack of a reference. These data show that nordenskiöldine is precipitated at stage 2, probably from a fluid enriched in boron by fractional crystallization.

5. Conclusions

Our investigation by the PIXE-PIGE method of geologically well characterized minerals and related FI from various crustal environments shows: (1) Geochemical anomalies observed in whole rock analyses are also present in individual minerals analysed at a micrometer-scale, provided that these minerals are the only phases containing the elements. (2) Measuring light and trace elements in solids is a useful tool for characterizing unusual (micro)phases, to constrain the relationship between minerals in a paragenetic sequence (co-precipitation, replacement, etc.), and to determine their formation temperatures. (3) PIXE-PIGE analyses are complementary to Raman microspectrometry, because the former method identifies elements whereas the latter is sensitive to chemical bonds. (4) For FI, major limitations to routine analysis by the PIXE-PIGE method are the accurate estimation of their depth in crystals, and the availability of optical systems that allow simultaneous viewing of the beam and μm-wide targets in transmitted light.

Acknowledgements

We are very grateful to the teams of the CERI-CNRS and LPS-CEA-CNRS laboratories for their technical assistance and friendly reception. We want to acknowledge particularly Pr Didier Isabelle, who died two years ago, for showing us the potentialities of the nuclear probe and for efficiently initiating us in its use. We also thank an unknown reviewer for his critical comments and Pr Mc Donald from Lancaster University for improving the writing of the paper.

References

[1] A.J. Anderson, A.H. Clark, X.P. Ma, G.R. Palmer, J.D. MacArthur, Econ. Geol. 84 (1989) 924.
[2] C.G. Ryan, C.A. Heinrich, T.P. Mernagh, Nucl. Instr. and Meth. B 77 (1993) 463.
[3] E. Zine, D.B. Isabelle, G. Rémond, Nucl. Inst. and Meth. B 49 (1990) 446.
[4] G. Rémond, C. Gilles, D. Isabelle, C.G. Choi, M. Azahra, O. Rouer, F. Cesbron, Appl. Radiat. Isot. 46 (1995) 563.
[5] G. Revel, J.P. Duraud, Technique de l'Ingénieur 10 (1995) 1.
[6] J.A. Maxwell, W.J. Teesdale, J.L. Campbell, Nucl. Instr. and Meth. B 95 (1995) 407.
[7] C.G. Ryan, D.R. Cousens, C.A. Heinrich, W.L. Griffin, S.H. Sie, T.P. Mernagh, Nucl. Instr. and Meth. B 54 (1991) 292.
[8] C.G. Choi, Thesis Univ. Orléans (1996).
[9] M. Edon, C. Ramboz, M. Volfinger, C.G. Choi, D. Isabelle, C.R. Acad. Sci. Paris 322 (1996) 633.
[10] L.A. Hardie, Contrib. Mineral. Petrol. 82 (1983) 205.
[11] M. Volfinger, J.L. Robert, J. Radioanal. Nucl. Chem. 185 (1994) 273.
[12] K. Ishii, M. Valladon, J.L. Debrun, Nucl. Instr. and Meth. B 150 (1978) 213.
[13] E. Oudin, in: Marine Minerals, eds. P.G. Teleki, M.R. Dobson, J.R. Moore, U. von Stackelberg (Reidel, Dordrecht, 1987) p. 349.
[14] Y. Fouquet, U. von Stackelberg, J.L. Charlou, J. Erzinger, P.M. Herzig, R. Mühe, M. Wiedicke, Econ. Geol. 88 (1993) 2154.
[15] T.M. Seward, Econ. Geol. Monograph 6 (1989) 398.
[16] M.D. Hannington, S.D. Scott, Econ. Geol. 6 (1989) 491.
[17] C. Marignac, C. Lécuyer, M. Dubois, Y. Fouquet, C. Ramboz, Terra Nova 1 (1995) 211.

[18] C. Ramboz, E. Oudin, Y. Thisse, Canad. Mineral. 26 (1988) 765.
[19] P.M. Herzig, M.D. Hannington, Y. Fouquet, U. von Stackelberg, S. Petersen, Econ. Geol. 88 (1993) 2182.
[20] E. Oudin, Y. Thisse, C. Ramboz, Mar. Geol. 5 (1984) 3.
[21] C. Ramboz, M. Danis, E. Oudin and Y. Thisse, Plinius 5 (1991) 182, Supplemento italiano Eur. J. Mineral.
[22] V. Marchig, H. Puchelt, H. Rösch, N. Blum, Marine Mining 9 (1990) 459.
[23] Ph. Sonnet, J. Verkaeren, Econ. Geol. 84 (1989) 575.
[24] M. Aissa, C. Ramboz, C. Bény, M.L. Pascal, Boletin de la Sociedad Espanola de Mineralogia 18 (1995) 1.
[25] P.A. Candela, Reviews in Econ. Geol. 4 (1989) 203.